Diagnostic Utility of a Custom 34-Gene Anchored Multiplex PCR-Based Next-Generation Sequencing Fusion Panel for the Diagnosis of Bone and Soft Tissue Neoplasms With Identification of Novel *USP6* Fusion Partners in Aneurysmal Bone Cysts

Josephine K. Dermawan, MD, PhD; Yu Wei Cheng, PhD; Zheng Jin Tu, PhD; Anders Meyer, MD; Omar Habeeb, MD; Youran Zou, MD; John R. Goldblum, MD; Steven D. Billings, MD; Scott E. Kilpatrick, MD; John D. Reith, MD; Sheila A. Shurtleff, PhD; Daniel H. Farkas, PhD; Brian P. Rubin, MD, PhD; Elizabeth M. Azzato, MD, PhD

• ***Context.***—**Bone and soft tissue tumors are heterogeneous, diagnostically challenging, and often defined by gene fusions.**

Objective.—**To present our experience using a custom 34-gene targeted sequencing fusion panel.**

Design.—**Total nucleic acid extracted from formalin-fixed, paraffin-embedded (FFPE) tumor specimens was subjected to open-ended, nested anchored multiplex polymerase chain reaction and enrichment of 34 gene targets, thus enabling detection of known and novel fusion partners.**

Results.—**During a 12-month period, 147 patients were tested as part of routine clinical care. Tumor percentage ranged from 10% to 100% and turnaround time ranged from 3 to 15 (median, 7.9) days. The most common diagnostic groups were small round blue cell tumors, tumors of uncertain differentiation, fibroblastic/myofibroblastic tumors, and adipocytic tumors. In-frame fusion transcripts were identified in 64 of 142 cases sequenced (45%): in 62 cases, the detection of a disease-defining fusion confirmed the morphologic impression; in 2 cases, a germline *TFG-GPR128* polymorphic fusion variant was detected. Several genes in the panel partnered with multiple fusion partners specific for different diagnoses, for example, *EWSR1*, *NR4A3*, *FUS*, *NCOA2*, and *TFE3*. Interesting examples are presented to highlight how fusion detection or lack thereof was instrumental in establishing accurate diagnoses. Novel fusion partners were detected for 2 cases of solid aneurysmal bone cysts (*PTBP1-USP6*, *SLC38A2-USP6*).**

Conclusions.—**Multiplex detection of fusions in total nucleic acid purified from FFPE specimens facilitates diagnosis of bone and soft tissue tumors. This technology is particularly useful for morphologically challenging entities and in the absence of prior knowledge of fusion partners, and has the potential to discover novel fusion partners.**

(*Arch Pathol Lab Med.* 2021;145:851–863; doi: 10.5858/arpa.2020-0336-OA)

Gene fusions occur frequently in bone and soft tissue (BST) neoplasms and, less frequently, in other kinds of solid tumors.[1–3] The observation of these fusions in patient specimens can assist in establishing a diagnosis or prognosis, and in potentially guiding therapy.[2,3] Recently, a few centers have reported the use of next-generation sequencing (NGS) for the detection of gene fusions as a diagnostic tool for BST tumors.[4–6] Anchored multiplex polymerase chain reaction (AMP) is particularly suited for detection of gene fusions in the absence of prior knowledge of the fusion partners.[7,8] Since many fusions specific to different morphologically similar BST entities share the same partners (eg, *EWSR1* fusions are common to both Ewing sarcoma and desmoplastic small round cell tumor), traditional techniques such as break-apart fluorescence in situ hybridization (FISH) do not distinguish these entities. On the other hand, within the same entity, the same gene could be associated with multiple partners (eg, *EWSR1-FLI1*, *EWSR1-ERG*, *EWSR1-FEV* for Ewing sarcoma),[9] and thus

Accepted for publication August 28, 2020.
Published online November 4, 2020.

From Robert J. Tomsich Pathology and Laboratory Medicine Institute, Cleveland Clinic, Cleveland, Ohio (Dermawan, Cheng, Tu, Goldblum, Billings, Kilpatrick, Reith, Shurtleff, Farkas, Rubin, Azzato); the Department of Pathology and Laboratory Medicine, University of Kansas Medical Center, Kansas City (Meyer); the Department of Anatomic Pathology, Middlemore Hospital, Counties Manukau District Health Board, Auckland, New Zealand (Habeeb); and the Department of Pathology, Kaiser Permanente Oakland Medical Center, Oakland, California (Zou).

The authors have no relevant financial interest in the products or companies described in this article.

An abstract based on this study was presented as a poster presentation at the 2019 Association for Molecular Pathology meeting; November 7–9, 2019; Baltimore, Maryland.

Corresponding author: Elizabeth M. Azzato, MD, PhD, Section of Molecular Genetic Pathology, Department of Laboratory Medicine, Robert J. Tomsich Pathology and Laboratory Medicine Institute, Cleveland Clinic, 9500 Euclid Ave, Cleveland, OH 44195 (email: azzatoe@ccf.org).

Table 1. The Genes (34), Transcripts, Directions, and Exons in the Bone and Soft Tissue Neoplasm Gene Fusion Next-Generation Sequencing–Based Laboratory-Developed Test

	Bone and Soft Tissue Neoplasm Gene Fusion Panel						
Gene	Transcript	Exon(s) Covered	Direction	Gene	Transcript	Exon(s) Covered	Direction
ALK	NM_004304.4	2, 4, 6, 10, 16–23, 25, 26	5′	*NTRK1*	NM_002529.3	2, 4, 6, 8, 10–13	5′
BCOR	NM_001123385.1	6, 7, 12, 14, 15	3′	*NTRK2*	NM_006180.4	5, 7, 9, 11–17	5′
BCOR	NM_017745.5	8	5′	*NTRK3*	NM_001007156.2	15	5′
BCOR	NM_001123385.1	7, 8	5′	*NTRK3*	NM_002530.3	4, 7, 10, 12–16	5′
CAMTA1	NM_015215.2	3	3′	*NTRK3*	NM_002530.3	13–15	3′
CAMTA1	NM_015215.2	8–10	5′	*NUT*	NM_175741.2	2, 3	5′
CCNB3	NM_033031.2	2–6	5′	*PAX3*	NM_181459.3	6, 7	3′
CIC	NM_015125.3	18–20	3′	*PAX3*	NM_181459.3	8	5′
CSF1	NM_000757.5	5–8	3′	*PDGFB*	NM_002608.2	2, 3	5′
CSF1	NM_172212.2	9	3′	*PLAG1*	NM_002655.2	1–4	5′
CSF1	NM_000757.5	6	5′	*ROS1*	NM_002944.2	2, 4, 7, 31–37	5′
EPC1	NM_025209.3	9–11	3′	*SS18*	NM_001007559.1	4–6, 8–10	3′
EWSR1	NM_005243.3	4–14	3′	*SS18*	NM_001007559.1	10, 11	5′
FOS	NM_005252.3	4	3′	*STAT6*	NM_001178078.1	1–7, 15–20	5′
FOSB	NM_006732.2	1, 2	3′	*TAF15*	NM_139215.2	5–7	3′
FOXO1	NM_002015.3	1–3	3′, 5′	*TAF15*	NM_139215.2	6, 7	5′
FUS	NM_004960.3	3–11, 13, 14	3′	*TCF12*	NM_207036.1	4–6	3′
GLI1	NM_005269.2	4–7	3′, 5′	*TFE3*	NM_006521.4	2–8	5′
HMGA2	NM_003483.4	1–5	3′	*TFE3*	NM_006521.4	2–6	3′
JAZF1	NM_175061.3	2–4	3′	*TFG*	NM_006070.5	3–7	3′
MEAF6	NM_001270875.1	4, 5	3′	*TFG*	NM_006070.5	6	5′
MKL2	NM_014048.4	11–13	5′	*USP6*	NM_004505.3	1–3	5′
NCOA2	NM_006540.3	11–16	5′	*YWHAE*	NM_006761.4	5	3′

reverse transcription–polymerase chain reaction (RT-PCR) is not possible without knowing the identity of both partners.

Our laboratory-developed test (LDT), termed *Sarcoma Testing by Next-Generation Sequencing* (SRCNGS), is a 34-gene, custom-designed, targeted sequencing panel for BST tumors. This anchored multiplex PCR-based test is used to detect the presence of fusion transcripts in targeted regions of total nucleic acid (TNA) isolated from formalin-fixed, paraffin-embedded (FFPE) tissue specimens. The TNA is then subjected to nested multiplex PCR enriching 34 gene targets before massively parallel sequencing with 151×2 cycle paired-end reads. We demonstrate the diagnostic utility of this LDT for a large prospective series of cases, submitted for clinical sequencing for a 1-year period, featuring examples of challenging and interesting BST neoplasms to highlight how fusion detection or lack thereof can be instrumental in establishing an accurate diagnosis. We also present the detection of a germline in-frame gene fusion, *TFG-GRP128*, in 2 cases (1.3% of test population, of 145 cases), which represents a population variant that should not be interpreted as a somatic gene fusion product. Finally, we report the discovery of novel fusion partners of *USP6* in 2 cases of aneurysmal bone cysts, illustrating how AMP-based NGS could lead to discoveries of novel translocation partner genes in BST neoplasms.

MATERIALS and METHODS

Total Nucleic Acid Extraction From FFPE

Five to 10 unstained slides and 1 hematoxylin-eosin (H&E)–stained slide from neutral buffered FFPE tissue sectioned at 4 μm were obtained from each specimen. FFPE samples were transported and stored at room temperature. A pathologist circled the area of interest on the H&E slide to enrich tumor purity from the harvested FFPE slides and avoid possible areas with necrosis or extensive hemorrhage. In addition, the percentage of tumor cells estimated to be present in the marked area of interest was provided to the laboratory, with a minimum of 10% tumor purity required. After deparaffinization with xylene, each slide underwent microdissection using a light microscope to capture the cellular areas of interest for molecular testing. Total nucleic acid extraction was performed by using the Maxwell RSC FFPE Kits (catalog Nos. AS1440 and AS1450, Promega) and protocol on the Maxwell RSC instrument. Total nucleic acid was quantified by using both the Qubit Ribonucleic acid (RNA) HS Assay Kit (catalog No. Q32852, Invitrogen) and Nanodrop 8000 spectrophotometer (ThermoFisher). Optimally, 200 ng of extracted TNA in 20 μL of ultrapure water (Archer kit No. SA0213, Archer DX Inc, Boulder, Colorado) was used for the assay (minimum input, 50 ng TNA).

Anchored Multiplex PCR

Total nucleic acid was converted to complementary DNA (cDNA) and evaluated with the Archer PreSeq RNA Quality Control (QC) assay, a quantitative PCR (qPCR) method to assess initial RNA quality. If satisfactory for testing (PreSeq qPCR crossing point < 30), cDNA libraries were made by using anchored multiplex PCR (Archer FusionPlex standard protocol and reagents) and custom-designed gene-specific primer (GSP) pools, targeting the 34 genes included in this panel that are involved in BST tumors. A total of 242 unidirectional GSPs were used to enrich TNA for known and unknown fusion transcripts (Table 1).

Massively Parallel Sequencing

Sequencing was performed on the MiSeq instrument (Illumina, San Diego, California) with 151×2 cycle paired-end reads to a depth of more than 500 000 total reads. A reversible terminator "sequencing by synthesis" technology enabled detection of each nucleotide incorporated into a growing DNA strand. During each cycle, a single fluorescently labeled deoxynucleotide triphosphate (dNTP) was added to the growing nucleic acid chain. The labeled

Table 2. Clinical and Laboratory Summary	
Total No. of Cases	**147**
Sex	65 females, 82 males
Age, y	1–90; median, 45
Nucleic acid concentration, ng/μL	2.1–90.0; mean, 20.8
Tumor content, %	10–100; mean, 71.0
In-lab turnaround time, d	3–15; median, 7.9

nucleotide served as a terminator for polymerization and after each dNTP incorporation, the fluorescent dye was imaged to identify the base that was then enzymatically cleaved to allow incorporation of the next nucleotide. Adapters containing both molecular barcodes and sample indices enabled quantitative multiplex data analysis, read deduplication, and accurate variant calling. The maximum amount of samples to be sequenced on a MiSeq v3 standard cartridge run is 14. A single SRCNGS run can contain up to 12 patient specimens, 1 no-template negative control (ultrapure water, Archer kit No. SA0213), and 1 positive QC control specimen (Horizon Discover, Cambridge, United Kingdom; catalog No. HD796 positive control, which include the following fusions: *ETV6-NTRK3*, *SLC34A2-ROS1*, *EML4-ALK*, and *TPM3-NTRK1*). For each sequencing run, greater than 500 000 fragments were obtained.

Validation Summary

Our AMP-based NGS LDT, termed *Sarcoma Testing by Next-Generation Sequencing*, is based on a validation study including 87 specimens. Briefly, this LDT demonstrates the following analytic performance metrics: 98.7% accuracy based on concordance with previous results by NGS, break-apart FISH, RT-PCR, and immunohistochemistry; 100% precision across different instruments and during a 3-day period by different laboratory technologists; an analytic sensitivity (limit of detection) of 10% tumor purity; and 99% analytic specificity.

Informatics Pipeline and Gene Fusion Report Criteria

Results from Archer analysis software (version 6.0.3.2) and an in-house informatics pipeline were used for read alignment (genome build hg19/GRCh37), fusion gene identification, data visualization and annotation. Reporting criteria of a gene fusion were as follows: (1) a minimum of 5 unique reads spanning the fusion junction, (2) at least 3 unique start sites present among these unique reads, and (3) at least 10% of reads surrounding the breakpoint that supported the fusion event. Fusion genes that did not meet the above criteria could be reported if they had been previously documented and at molecular pathology professional staff discretion. A sample could be reported as "quality not sufficient" when the following quality metric circumstances were not met: (1) the number of unique RNA reads was less than 30% of total reads; and (2) the average number of RNA reads with unique start sites derived from the control GSP2 (gene-specific primer 2) was fewer than 10. All technical quality data and potential fusion reads were inspected by molecular pathology professional staff before clinical reporting. Fusions were evaluated for clinical reporting, based on several features, including whether the fusion had been previously reported, if the fusion product was predicted to be in-frame, configuration of the chimeric protein domains, and consideration of possible promoter swap.

RESULTS

Cohort Description and Diagnostic Utility of the Bone and Soft Tissue Gene Fusion Panel

Among the 147 cases (65 females, 82 males; aged 1–90 years [median, 45]) submitted for sequencing with the SRCNGS LDT, 142 (97%) passed quality control measures and were successfully sequenced. The cases that were submitted were selected by individual pathologists on a case-by-case basis on the basis of diagnostic needs. Tumor content ranged from 10% to 100%, with a mean nucleic acid concentration of 20.8 ng/μL. The average turnaround time was 7.5 days (Table 2). A fusion was observed in 64 of the 142 cases (45%) that were sequenced, confirming the diagnoses of 62 cases. Among the remaining 78 cases where no fusions were detected, 24 cases (32%) were diagnosed or an alternative diagnosis was favored, since morphologic mimics with a known recurrent fusion were ruled out. The remaining cases either remained unclassified (44 cases) or had a preexisting diagnosis that remained unchanged (10 cases) (Figure 1).

Gene Fusions Detected

The most commonly detected fusions were *EWSR1-FLI1* (Ewing sarcoma), *SS18-SSX2* (synovial sarcoma), *EWSR1-NR4A3* (extraskeletal myxoid chondrosarcoma, EMC), *FUS-DDIT3* (myxoid liposarcoma), and *CIC-DUX4* (Ewing-like sarcoma). Several genes in the panel, particularly *EWSR1*, demonstrated multiple partners detected by the LDT. For example: (1) *EWSR1* was detected with *FLI1*, *ERG*, and *FEV* for Ewing sarcoma, *NR4A3* for EMC, *CREB1* and *ATF1* for angiomatoid fibrous histiocytoma (AFH) and clear cell sarcoma (CCS), *CREB3L1* for low-grade fibromyxoid sarco-

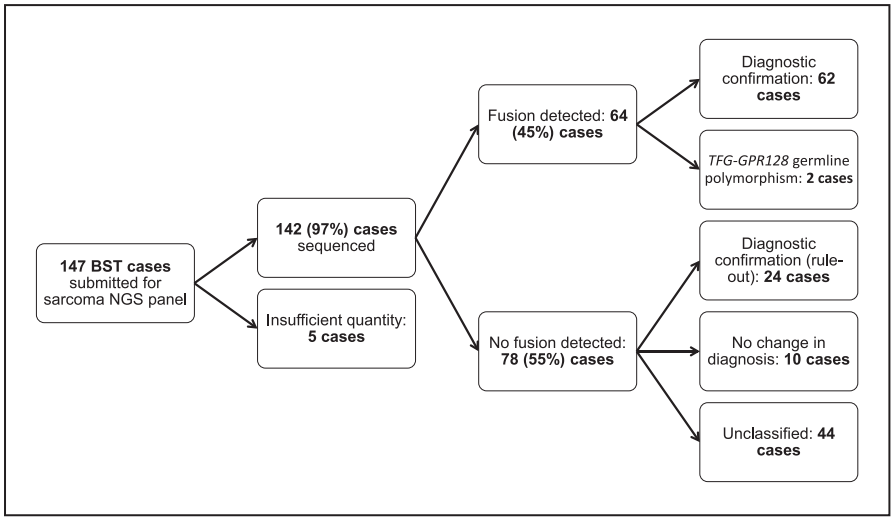

Figure 1. *Flowchart of cases diagnosed and classified by the Bone and Soft Tissue Gene Fusion Panel. Abbreviations: BST, bone and soft tissue; NGS, next-generation sequencing.*

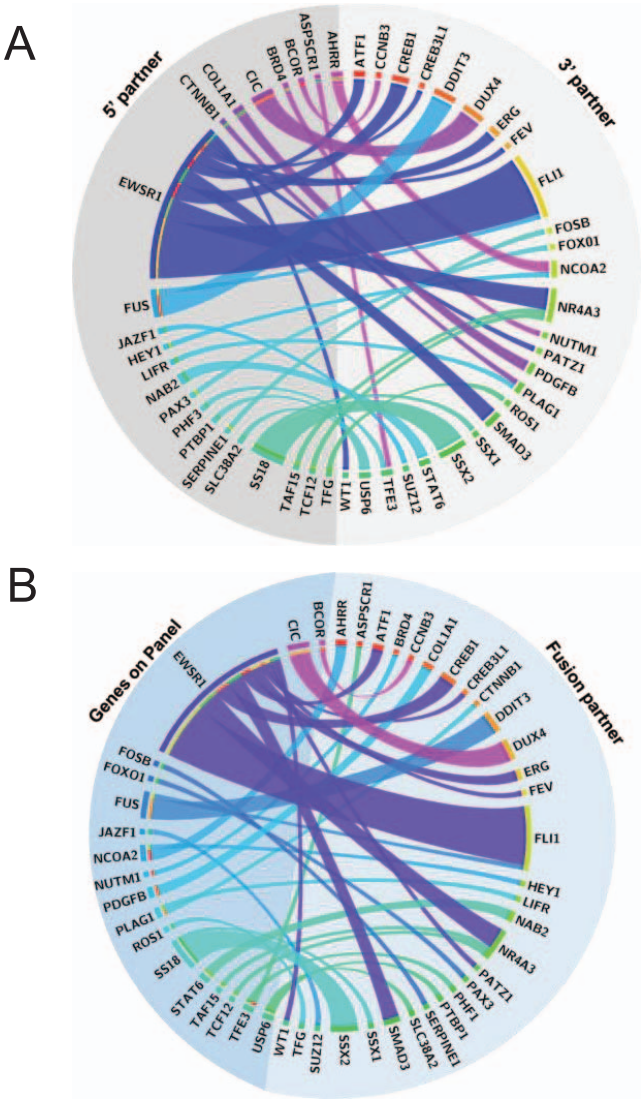

Figure 2. *Fusions detected by the Sarcoma Testing by Next-Generation Sequencing laboratory-developed test. A, A circos plot displaying fusions listed by 5′ and 3′ partners. B, A circos plot displaying fusions listed by genes in the LDT panel and their partners. The width of the ribbons on both circos plots is proportional to the number of fusions observed in our cohort.*[59]

ma (LGFMS) and sclerosing epithelioid fibrosarcoma, and *SMAD3* for *EWSR1-SMAD3*–rearranged acral fibroblastic tumor; (2) *FUS* was detected with *DDIT3* for myxoid liposarcoma and *FLI1* for Ewing sarcoma; (3) *NCOA2* was detected with *AHRR* for soft tissue angiofibroma and *HEY1* for mesenchymal chondrosarcoma; (4) *SS18* was detected with *SSX1* and *SSX2* for synovial sarcoma; and (5) *TFE3* was detected with *ASPSCR1* for alveolar soft part sarcoma and *PHF1* for ossifying fibromyxoid tumor (Figure 2, A and B).

Diagnostic Categories of Bone and Soft Tissue Entities

Among the 62 cases diagnosed by detection of fusions, the most common types of BST tumors diagnosed were small round blue cell tumors (n = 21, 34%; eg, Ewing sarcoma, Ewing-like sarcoma), tumors of uncertain differentiation/histogenesis (n = 15, 24%; eg, synovial sarcoma, extraskeletal myxoid chondrosarcoma), tumors of fibroblastic/myofibroblastic differentiation (n = 13, 21%; eg, angiomatoid fibrous histiocytoma, *EWSR1-SMAD3*–rearranged acral fibroblastic tumor, dermatofibrosarcoma protuberans, soft tissue angiofibroma, solitary fibrous tumor), and adipocytic tumors (n = 4, 6%; eg, myxoid liposarcoma). In addition to mesenchymal neoplasms, a small minority of cases were carcinomas with disease-defining fusions, for example, *BRD4-NUTM1* (midline) carcinomas and pleomorphic adenomas with *PLAG1* fusions (Figure 3, A and B).

Recurrent Germline *TFG-GPR128* Polymorphic Fusion

Although uncommon, polymorphic copy number and structural variation can lead to in-frame fusion products. One such described event is *TFG-GPR128*.[10,11] A germline copy number gain involving chromosome 3q12.2 results in an in-frame transcript fusing *TFG* exon 3 to *GPR128* exon 2.

In our cohort, 2 cases were detected (1.3% of tested population, of 147 cases). Case 1 was a retroperitoneal biopsy in a middle-aged male with a presumed diagnosis of Ewing sarcoma (85% tumor purity). In addition to the detection of a *FUS-FLI1* fusion (561 reads), which was diagnostic of Ewing sarcoma, a *TFG-GPR128* fusion was also detected (304 reads). Case 2 was a biopsy of a right flank mass in a middle-aged male with a presumed diagnosis of sclerosing epithelioid fibrosarcoma (SEF; 100% tumor purity). A *TFG-GPR128* fusion was detected (310 reads), while no somatic gene fusions were detected. In both cases, exon 3 of *TFG* (NM_006070; hg19 chr3:100438902) was fused to exon 2 of *GPR128* (NM_032787.2; hg19 chr3:100348442).

Examples of Entities Diagnosed by Detection of Disease-Defining Fusion

A number of round cell sarcoma entities are characterized by the presence of small round cells with scant cytoplasm and round nuclei: *FUS-FLI1*–rearranged Ewing sarcoma[9] (Figure 4, A), *CIC-DUX4*–rearranged round cell (Ewing-like) sarcoma[12] (Figure 4, B), *BCOR-CCNB3*–rearranged round cell (Ewing-like) sarcoma[13] (Figure 4, C), and *EWSR1-WT1*–rearranged desmoplastic small round cell tumor (DSRCT)[14] (Figure 4, D). Both Ewing and Ewing-like sarcomas show sheets of primitive, uniform small round blue cells, with only subtle morphologic differences (see Figure legend for details). Some DSRCTs could show only predominantly sheets of small round cells with scant cytoplasm and lack the characteristic desmoplastic stroma (Figure 4, D). Detection of a specific fusion is necessary to distinguish among these round cell sarcomas.

Soft tissue angiofibroma is composed of largely nondistinctive, bland spindle cells with a prominent, branching vasculature, occasional ectatic, "staghorn" vessels, and areas of loose, myxoid stroma to more collagenous areas. Its mimics include LGFMS, solitary fibrous tumor, and myxoid liposarcoma, which could be differentiated by detection of the *AHRR-NCOA2* fusion (Figure 4, E).[15]

Extraskeletal myxoid chondrosarcoma (EMC) could closely resemble myoepithelial neoplasms.[16] Overall, 5 cases of EMC were diagnosed in this series, 3 of which showed an *EWSR1-NR4A3* fusion, with 1 *TAF15-NR4A3* and *TCF-NR4A3* fusion each. In one instance, a *TCF12-NR4A3* fusion, the rarest of all EMC fusions,[17] was detected and confirmed the diagnosis of EMC (Figure 4, F).

Histologically, AFH is a well-circumscribed mass composed of uniform, bland, spindled to histiocytic tumor cells. It is often surrounded by a thick fibrous capsule, peripheral lymphoplasmacytic inflammation, and dilated blood-filled

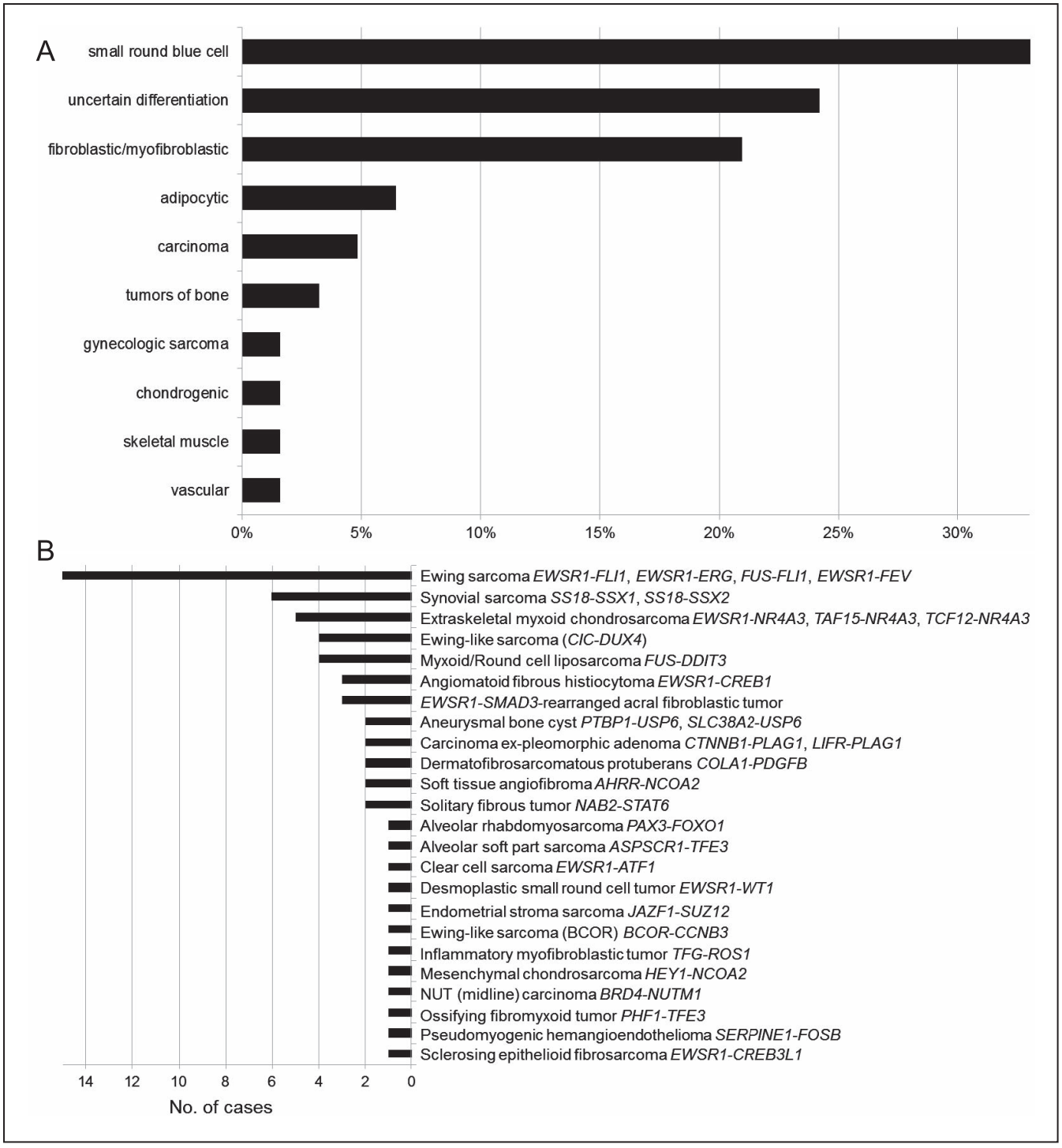

Figure 3. *A, Distribution of histologic categories of entities diagnosed by using a laboratory-developed test (LDT). B, Distribution of diagnoses and fusions confirmed by the LDT.*

cystic spaces. When only a limited biopsy sample is available (Figure 4, G), the characteristic features of the capsule, peripheral inflammation, and dilated blood-filled spaces can be absent, and the detection of the *EWSR1-CREB1* fusion is useful to rule out other diagnoses,[18] particularly a reactive process.

Inflammatory myofibroblastic tumor (IMT) is a variably cellular spindle cell lesion with a mixed inflammatory, largely lymphoplasmacytic infiltrate within a collagenous stroma. Immunohistochemically, ALK-negative IMTs are positive for smooth muscle actin and desmin, but negative for ALK1 staining.[19] Detection of non-ALK fusions, such as *TFG-ROS1* (Figure 4, H), could help confirm the morphologic impression of IMT and rule out a reactive process and other intraabdominal spindle cell tumors, such as gastrointestinal stromal tumor and fibromatosis.

SEF is composed of vague nests and cords of monomorphic, bland epithelioid cells with round nuclei and

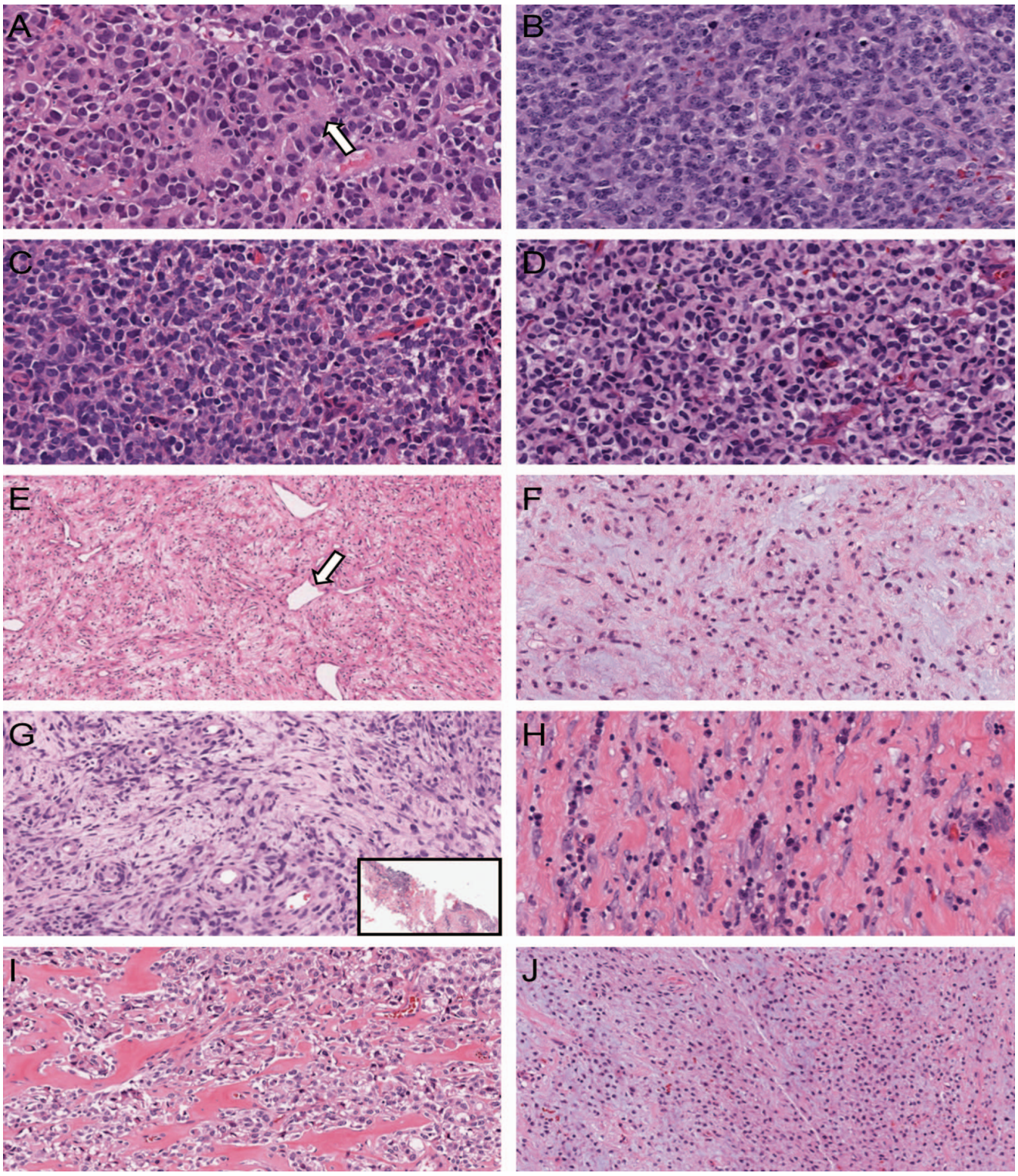

Figure 4. *Examples of entities diagnosed by detection of disease-defining fusions with the Sarcoma Testing by Next-Generation Sequencing laboratory-developed test. Fusions detected are indicated in parentheses. A, Ewing sarcoma (*FUS-FLI1*) composed of sheets of monotonous, closely packed cells with scant cytoplasm, small, round nuclei, finely granular chromatin, and inconspicuous nucleoli. Homer Wright rosettes (arrow) are readily seen. B, CIC-rearranged round cell (Ewing-like) sarcoma (*CIC-DUX4*) with uniform, packed cells with scant cytoplasm, slightly more irregular nuclei, and prominent nucleoli. No rosette formation is seen. C,* BCOR-rearranged round cell (Ewing-like) sarcoma (BCOR-CCNB3*) composed of small, round to ovoid tumor cells, with very similar morphology to Ewing sarcoma. D, Desmoplastic small round cell tumor (*EWSR1-WT1*) showing nests and sheets of small round cells with scant presence of myxoid matrix but without prominent desmoplastic stroma. E, Angiofibroma of soft tissue (*AHRR-NCOA2*) composed of relatively uniform, bland spindle cells in a variably myxoid to collagenous stroma. A prominent, thin-walled, branching vasculature is seen throughout the tumor. Occasional ectatic, hemangiopericytoma-like staghorn vessels (arrow) are also seen. F, Extraskeletal myxoid chondrosarcoma (*TCF12-NR4A3*) composed of epithelioid to spindled cells with round to ovoid nuclei and eosinophilic*

inconspicuous nucleoli growing between thick collagenous, and osteoid-mimicking bundles (Figure 4, I). SEF could mimic other entities with bland epithelioid cells such as ossifying fibromyxoid tumor (OFMT), but could be diagnosed with MUC4 immunostaining or the presence of a *EWSR1-CREB3L1* fusion.[20] On the other hand, the diagnosis of "nonossifying" OFMT, usually implying OFMTs without a peripheral rim of ossification, could be challenging. OFMTs are characterized by the presence of *PHF1* fusions. In our series, a *PHF1-TFE3* fusion was detected (Figure 4, J), which was reported in a subset of OFMTs that behaves in a more aggressive fashion.[21]

Examples of Morphologic Mimics Differentiated by the Presence or Absence of Fusion

Tumors sharing a "fibrosarcomatous" pattern—spindle cells arranged in tight fasicles with a herringbone appearance—could pose a diagnositic challenge. For example, dermatofibrosarcoma protuberans (DFSP) could undergo fibrosarcomatous transformation, which could lose CD34 immunostaining, but may be diagnosed with detection of *COL1A1-PDGFB* (Figure 5, A).[22] In contrast, the absence of a detectable fusion could sometimes help support the diagnosis of a malignant peripheral nerve sheath (MPNST) tumor (Figure 5, B) by excluding a diagnosis of synovial sarcoma, which has significant histologic overlap with MPNST.[23]

Both CCS and malignant melanoma are characterised by melanocytic differentiation. Clear cell sarcoma consists of bundles and short fascicles of uniform, spindled to epithelioid cells with abundant eosinophilic cytoplasm; vesicular nuclei; and prominent, single nucleoli (Figure 5, C). Malignant melanomas are characterized by a diverse morphologic spectrum, some of which could show an almost identical morphology with CCS (Figure 5, D). Both entities also share identical immunohistochemical profiles (positivity for S100, SOX10, HMB-45, Melan-A). The detection of *EWSR1-ATF1* helps to establish the diagnosis of CCS and exclude a diagnosis of melanoma,[24] while the absence of a fusion could help support the diagnosis of melanoma and rule out CCS.[25,26]

When defining morphologic features are focal, tumors with lipoblastic differentiation could be challenging to differentiate. In some cases of high-grade myxoid liposarcoma (formerly known as round cell liposarcoma), the tumor could lack the more hypocellular, myxoid areas with plexiform vasculature that are characteristic of myxoid liposarcoma, which is the lower-grade form of high-grade myxoid liposarcoma, and contain predominantly hypercellular areas with small round cells (Figure 5, E). Areas with adipocytic differentiation, specifically lipoblasts, could be focal. The detection of *FUS-DDIT3* helps to establish the diagnosis of a high-grade myxoid liposarcoma and rule out other high-grade round cell sarcomas.[27] On the other hand, some pleomorphic liposarcomas could lack the characteristic extreme cytologic pleomorphism that is typical of this entity (Figure 5, F). The lack of a fusion can help rule out an unusual high-grade myxoid liposarcoma.[28]

Mesenchymal chondrosarcomas and the small cell variant of osteosarcomas are 2 bone tumors that can show nests of primitive, small round cells. Mesenchymal chondrosarcomas are characterized by cellular areas of primitive-appearing, round to ovoid cells with areas of mature hyaline cartilage (Figure 5, G). The detection of the *HEY1-NCOA2* fusion can help confirm the diagnosis of mesenchymal chondrosarcoma and rule out small cell or chondroblastic osteosarcoma and Ewing sarcoma.[29] On the other hand, small cell osteosarcomas can also show islands of primitive, small round cells with osteoid matrix and cartilage deposition (Figure 5, H), a morphology seen in both chondroblastic/small cell osteosarcoma and mesenchymal chondrosarcoma, the latter of which could be excluded by the absence of fusions.[30]

The entities for which a diagnosis was favored by the absence of detectable fusions, thus ruling out a morphologic mimic with a known fusion, are summarized in Table 3.

Novel *UPS6* Fusion Partners in Aneurysmal Bone Cysts

Aneurysmal bone cysts (ABCs) are known to harbor recurrent *USP6* translocations. To date, a number of fusion gene partners have been described, including *COL1A1*, *OMD*, *PAFAH1B1*, *RUNX2*, *SPARC*, *TRAP150*, *USP9X*, and *ZNF9*.[31–35] Figure 6 highlights 2 cases of solid ABC with *PTBP1-USP6* and *SLC38A2-USP6* translocations, respectively. The first case (Figure 6, A and B) is a biopsy from the left pelvic pubic ramus of a child. In a background of mostly normal trabecular bone and marrow elements, there is scant amount of lesional material with uniform and bland spindled cells, admixed with osteoclast-type giant cells and variable amounts of osteoid and bone rimmed by osteoblasts. Relative to the size of the lesion on radiology, the differential diagnosis was between a primary ABC versus a primary bone neoplasm with a secondary ABC component. The second case (Figure 6, C and D) is an excision of a right lower arm mass from a young male. Radiographs demonstrate a circumscribed lesion involving the volar surface of the radius with a circumferential rim of reactive bone. On magnetic resonance imaging, the lesion shows a lobular configuration, involves the adjacent medullary cavity, and extends into the adjacent muscle in a mushroom-like fashion, focally showing fluid-fluid levels. Histologic sections show a lobular, giant cell–rich spindle cell neoplasm with foci of reactive bone showing osteoblastic rimming, and scattered serpiginous and round blood lakes. Mitoses are easily identified without significant cytologic atypia. Immunohistochemically, the neoplastic cells were negative for H3G34W, G34R, and G34V histone antibodies. This was finally diagnosed as a case of solid ABC with the

←
*cytoplasm, arranged as single cells, cords, or clusters embedded in myxoid stroma. G, Angiomatoid fibrous histiocytoma (*EWSR1-CREB1*) composed of bland, ovoid, histiocyte-like short spindle cells with abundant pale eosinophilic cytoplasm and indistinct cell borders. The edge of this limited biopsy sample, as demonstrated by the inset, showed merely hints of the characteristic thick fibrous capsule and peripheral lymphoid tissue. Blood-filled cystic spaces were not identified. H, Inflammatory myofibroblastic tumor (*TFG-ROS1*) composed of variably cellular fascicles of uniform, plump spindle cells with elongated, tapering nuclei and ill-defined cell borders. A prominent infiltrate of lymphocytes and plasma cells is seen. This case is negative for ALK immunohistochemical staining, reflecting the lack of* ALK *gene fusions. I, Sclerosing epithelioid fibrosarcoma (*EWSR1-CREB3L1*) composed of vague nests and cords of monomorphic, bland epithelioid cells with round nuclei and inconspicuous nucleoli growing between thick collagenous, osteoid-mimicking bundles. J, A "nonossifying" ossifying fibromyxoid tumor (*PHF1-TFE3*) consisting of nests and cords of round to oval, epithelioid cells with indistinct cytoplasm embedded in a fibromyxoid matrix. A peripheral rim of ossification is absent (hematoxylin-eosin, original magnifications ×40 [A through D], ×10 [E], ×20 [F through J], and ×4 [inset G]).*

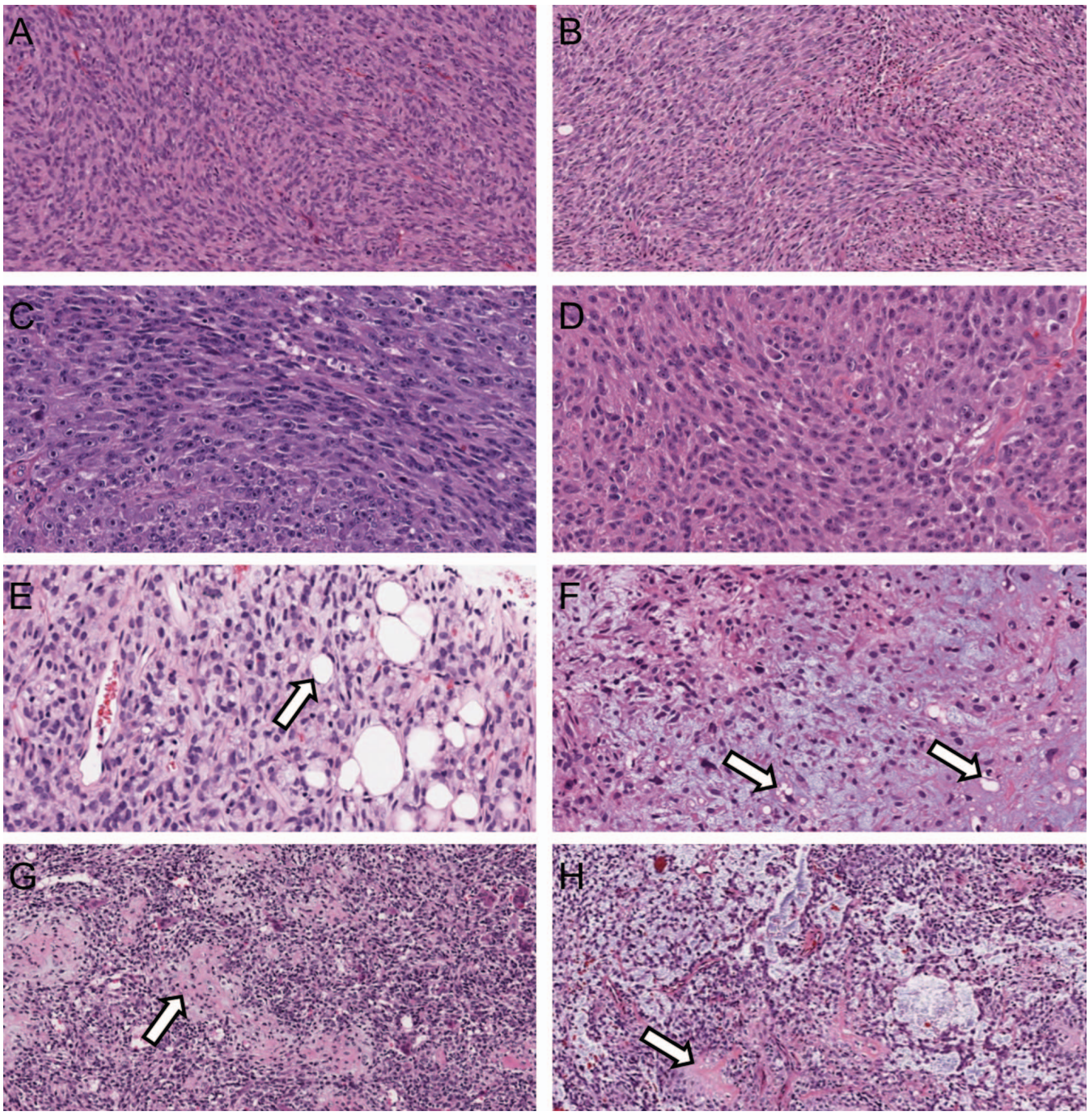

Figure 5. *Pairs of morphologically similar tumors with or without recurring fusions diagnosed with the assistance of the Sarcoma Testing by Next-Generation Sequencing laboratory-developed test. Fusions detected are indicated in parentheses. A, Dermatofibrosarcoma protuberans with fibrosarcomatous transformation (DFSP) (*COLA1-PDGFB*) with a uniformly fibrosarcoma-like fascicular growth pattern and lacking the typical storiform architecture that is seen in conventional DFSP. B, Malignant peripheral nerve sheath tumor (no known recurring fusions) composed of highly cellular, tight intersecting fascicles, similar to (A). The spindle cells are monotonous with indistinct cell borders, pale eosinophilic cytoplasm, and hyperchromatic, slender nuclei. C, Clear cell sarcoma (*EWSR1-ATF1*) composed of short fascicles of uniform spindle to epithelioid cells with eosinophilic cytoplasm, vesicular nuclei with prominent nucleoli. D, Melanoma (no known recurring fusions), spindled to epithelioid variant, with essentially identical morphologic features and immunophenotypic profile as (C). Both are positive for melanocytic markers including S100 and HMB-45. E, High-grade myxoid liposarcoma (*FUS-DDIT3*), a rare variant of myxoid liposarcoma in which hypercellularity and round cell morphologic features account for more than 80% of tumor tissue. Univacuolated lipoblasts (arrow) are present. F, Pleomorphic liposarcoma (no known recurring fusions) composed of pleomorphic, epithelioid to ovoid tumor cells with cellular atypia. Lipoblastic differentiation (arrows) is seen focally. G, Mesenchymal chondrosarcoma (*HEY1-NCOA2*) composed of primitive, cellular proliferation of round to ovoid cells with areas of mature, calcified, hyaline cartilaginous nodules (arrow). H, Small cell osteosarcoma (no known recurring fusions) composed of small, round cells with focal areas of lacelike osteoid formation (arrow) (hematoxylin-eosin, original magnifications ×10 [A, B, G, and H] and ×20 [C through F]).*

Table 3. Diagnoses Favored by Negative Fusions	
Diagnoses Favored by Negative Fusions	**Differential Diagnoses (Morphologic Mimic) Ruled Out**
Benign epithelioid angiomatous nodule	Epithelioid hemangioma
Carcinoma	Ewing-like sarcoma
Cellular fibrous histiocytoma	DFSP
Chondroid lipoma	Myxoid/round cell liposarcoma
Embryonal rhabdomyosarcoma	Alveolar rhabdomyosarcoma
Fibroinflammatory lesion	IMT
Hemangioma	EHE
Hemangioendothelioma, not otherwise specified	EHE
Intravascular angioma	EHE
Low-grade myofibroblastic sarcoma	IMT
Malignant extrarenal rhabdoid tumor	High-grade round cell sarcomas
Malignant melanoma	Gastrointestinal neuroectodermal tumor; clear cell sarcoma
Malignant peripheral nerve sheath tumor	Synovial sarcoma
Myofibroma	IMT; nodular fasciitis
Osteosarcoma (chrondroblastic)	Mesenchymal chrondrosarcoma
Osteosarcoma (osteoblastoma-like)	Osteoblastoma
Perineurioma	DFSP, low-grade fibromyxoid sarcoma
Pleomorphic liposarcoma	Myxoid/round cell liposarcoma
Soft tissue chondroma	EHE
Spindle cell lipoma	Myxoid DFSP

Abbreviations: DFSP, dermatofibrosarcoma protuberans; EHE, epithelioid hemangioendothelioma; IMT, inflammatory myxofibroblastic tumor.

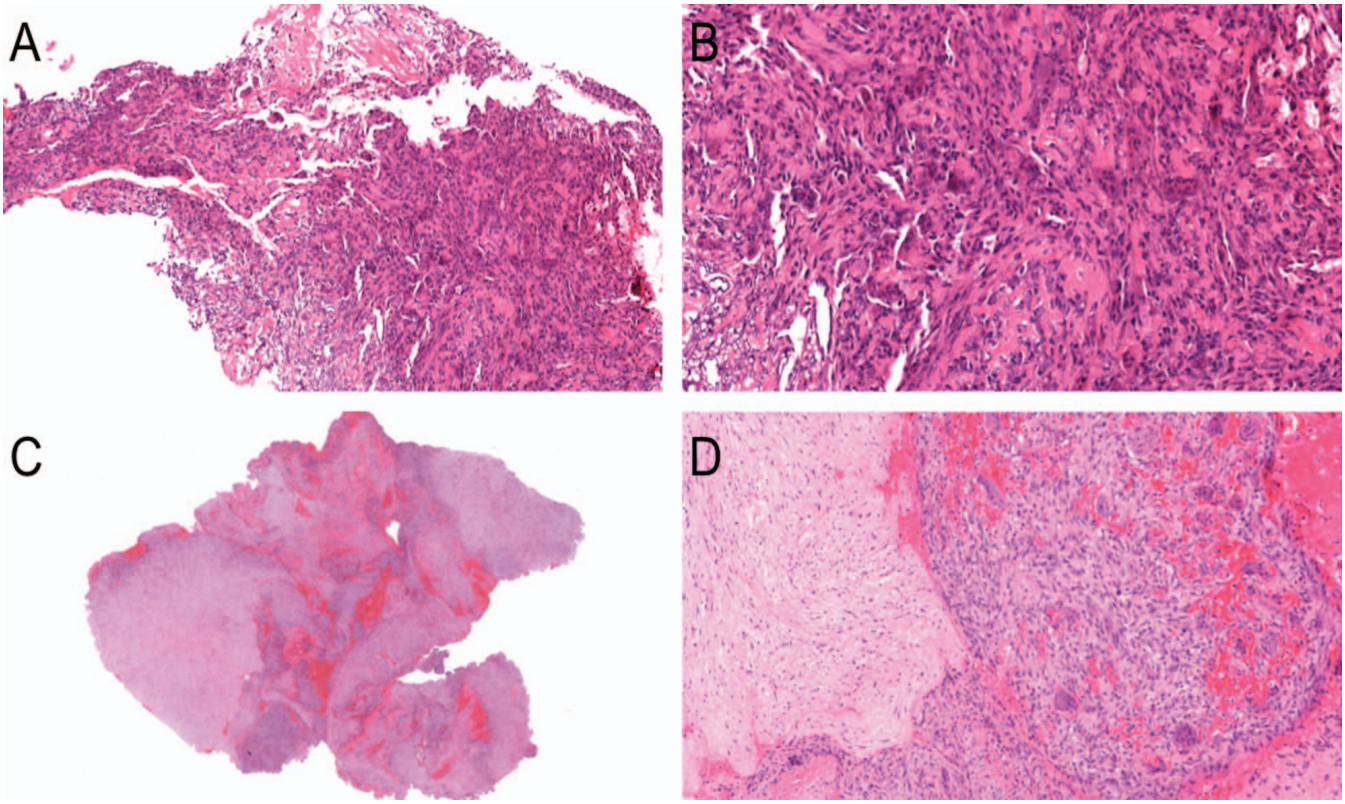

Figure 6. *Novel fusion partners diagnosed with the Sarcoma Testing by Next-Generation Sequencing laboratory-developed test. Two examples of solid aneurysmal bone cysts (ABCs) with* PTBP1-USP6 *(A and B) and* SLC38A2-USP6 *(C and D), respectively. A and B, The first case is a biopsy sample with scant amount of lesional material showing uniform, bland spindled cells admixed with osteoclast-type giant cells and variable amounts of osteoid and bone rimmed by osteoblasts. The differential diagnosis is between a primary ABC versus a primary bone neoplasm with a secondary ABC component. C and D, The second case is an excision specimen of a lobular, giant cell–rich spindle cell neoplasm with foci of reactive bone showing osteoblastic rimming, and scattered serpiginous and round blood lakes. Numerous mitoses but no significant cytologic atypia are identified. Despite being a circumscribed lesion with focal fluid-fluid levels on imaging, radiologic features were concerning for involvement of the adjacent medullary cavity and extension into the adjacent muscle in a mushroom-like fashion (hematoxylin-eosin, original magnifications ×10 [A and D], ×20 [B], and whole slide image [C]).*

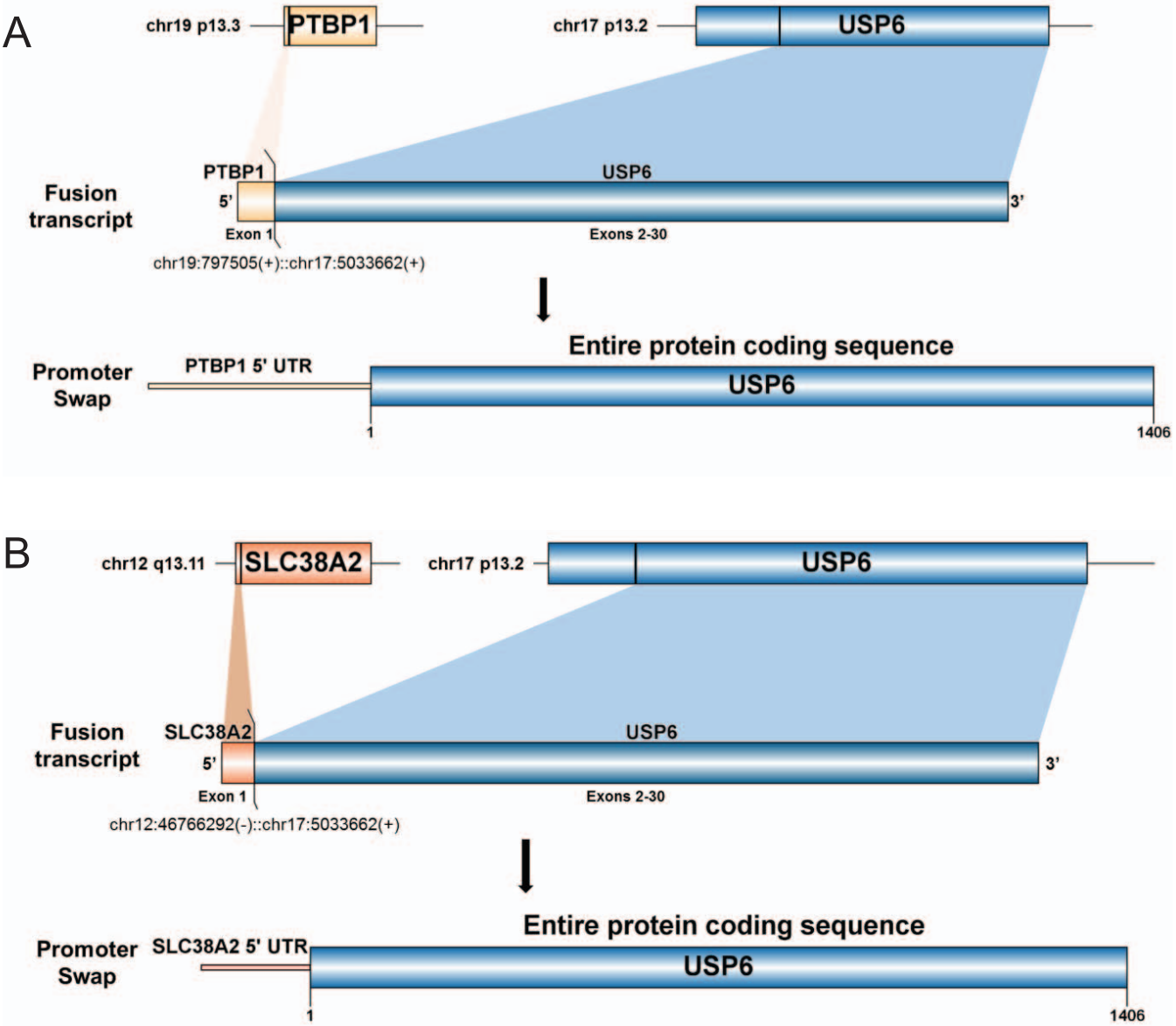

Figure 7. *A and B, Schematic of the detected* PTBP1-USP6 *[chr19:797505(+)::chr17:5033662(+)] and* SLC38A2-USP6 *[chr12:46766292(-)::chr17:5033662(+)] gene fusions. Both gene fusions result in fusion transcripts that include the exon 1 of* PTBP1 *(NM_002819.4) and that of* SLC38A2 *(NM_018976), respectively, fused to exons 2 to 30 of* USP6 *(NM_004505). The presumed mechanism is promoter swapping, similar to prior reports,[31] since exon 1 of both* PTBP1 *and* SLC38A2 *only encodes for 5′ untranslated regions (UTRs), while* USP6 *exons 2 to 30 encode for the entire protein coding sequence of USP6. Chromosomal positions are from the hg19 genome assembly.*

detection of an *SLC38A2-USP6* fusion. Both cases involved fusions with exon 2 of *USP6* (Figure 7, A and B). To our knowledge, these are novel gene fusion partners of *USP6* in ABC that have not yet been reported.

DISCUSSION

We present our clinical experience using a custom 34-gene targeted sequencing fusion panel LDT for BST neoplasms. We demonstrated successful sequencing in most cases (97%, 142 of 147 cases), with clinically useful turnaround times (~7 days), using as little as 50 ng of TNA extracted from FFPE tissue. A major advantage of this test is its ability to detect fusions even when the fusion partners not included in the panel are present in the tumor. Several genes in the panel, particularly *EWSR1*, had multiple partners that were detected. In fact, *EWSR1*, *FUS*, and *TAF15* are closely related genes that encode RNA-binding proteins.[36,37] All 3 genes, especially *EWSR1* and *FUS*, form fusion oncogenes that drive many types of distinct, unrelated BST tumors including Ewing sarcoma, AFH and CCS, LGFMS and SEF, *EWSR1-SMAD3*–rearranged acral fibroblastic tumor, and myxoid liposarcoma.[38–41] This illustrates the advantage of having the capacity to detect fusions when 1 partner is unknown, which significantly expands the ability of this 34-gene panel to detect a much higher number of possible fusions.

There is substantial morphologic and immunohistochemical overlap among Ewing sarcoma and Ewing-like sarcomas: CD99 is not specific to Ewing sarcoma and can show positivity in a large majority of *CIC*-rearranged sarcomas.[9] Similarly, SATB2 expression cannot be used to distinguish soft tissue involvement by small cell osteosarcoma, since

this marker tends to also show positivity in *BCOR*-rearranged Ewing-like sarcoma.[13] Since *CIC*-rearranged sarcoma is clinically more aggressive than Ewing sarcoma, distinguishing between these 2 entities is essential.[12] Interestingly, in the case of Ewing sarcoma, a *FUS-FLI1* fusion was detected; even though both partners have been reported in the Ewing family of tumors, this specific combination has not been reported to date in Ewing sarcoma.[9] When DSRCT lacks the characteristic prominent desmoplastic stroma, as in our case, it can be difficult to distinguish from Ewing sarcoma or other small round blue cell tumors.[14] Detection of *EWSR1* rearrangements by a break-apart FISH probe would not help differentiate DSRCT from Ewing sarcoma, since *EWSR1* could be a partner in both the disease-defining fusions for DSRCT (*EWSR1-WT1*) and Ewing sarcoma (*EWSR1* or *FUS* fusions). While immunohistochemical detection of cytokeratins, desmin, and WT1 (N terminal) is a useful adjunct to the distinction of DSRCT from Ewing sarcoma, detection of fusions by NGS is highly useful for definitive diagnosis of these tumors.

Soft tissue angiofibroma shows significant morphologic overlap with a number of low-grade BST tumors: (1) low-grade fibromyxoid sarcoma, which can also show alternating collagenous and myxoid areas; (2) myxoid liposarcoma, which is also characterized by a prominent plexiform vascular network; and (3) solitary fibrous tumor, which also contains staghorn vessels, as were present in our case. Detection of the *AHRR-NCOA2* fusion confirms the diagnosis of soft tissue angiofibroma.[13]

Both EMC and myoepithelial neoplasms are characterized by cords or isolated epithelioid cells embedded in myxoid stroma. EMC commonly harbors *EWSR1-NR4A3* gene fusions,[16] and *EWSR1* fusions have been observed in up to 50% of myoepithelial neoplasms.[17] Thus, detection of *EWSR1* rearrangements by a break-apart FISH probe does not help distinguish between the two. Further, a subset of EMC harbors *TAF15-NR4A3* and *TCF12-NR4A3* fusions,[14] which would be missed by *EWSR1* FISH alone. Among the 5 cases of EMC in our series, the most commonly detected fusion, similar to previous reports,[17] was *EWSR1-NR4A3*, followed by *TAF15-NR4A3* and *TCF12-NR4A3*.

Certain BST tumors are characterized by the presence of prominent inflammatory cells. One example is AFH, which is a well-circumscribed tumor composed of nodules of bland histiocytoid cells with a peripheral fibrous pseudocapsule containing a prominent lymphoplasmacytic infiltrate, which can be mistaken for a lymph node. Dilated, blood-filled pseudovascular spaces may also be present. Thus, the diagnosis of AFH can be challenging in a limited biopsy sample when the periphery is absent and only the histiocytoid tumor cells with scant inflammatory infiltrate are seen. The presence of the *EWSR1-ATF1* or *EWSR1-CREB1* fusion confirms the diagnosis of AFH and rules out a reactive process.[18] Another BST tumor with a prominent inflammatory infiltrate is IMT. The differential diagnosis of IMT is broad and may include various spindle cell sarcomas, particularly low-grade myofibroblastic sarcoma, inflammatory leiomyosarcoma, spindle cell gastrointestinal stromal tumor, fibromatosis, schwannoma, dendritic cell sarcomas, and reactive processes. Though it is classically immunopositive for ALK, only about 50% of IMTs are positive for *ALK* gene fusions, with a minor subset (5%–10%) harboring a fusion involving *ROS1*.[19]

In the absence of storiform areas that are characteristic of classical DFSP, the differential diagnosis of fibrosarcomatous DFSP is broad and includes spindle cell melanoma, spindle cell carcinoma, MPNST, and synovial sarcoma.[22] Monophasic synovial sarcoma shows significant overlap of histologic and immuophenotypic features with MPNST.[23] Fibrosarcomatous DFSP, monophasic synovial sarcoma, and MPNST can all show tight fascicles of spindle cells forming a herringbone pattern. Despite reports of using loss of H3K27 trimethylation as a diagnostic marker for MPNST,[42] this marker lacks specificity for MPNST in some laboratories.[43] More recently, loss of H3K27 dimethylation was proposed as a highly specific marker,[44] but the applicability of this marker remains to be seen due to its low sensitivity. Therefore, demonstration of specific fusion genes, that is, *COL1A1-PDGF* for DFSP and *SS18-SSX* fusions for synovial sarcoma, or lack thereof in the case of MPNST, is useful to differentiate among these tumors.

Clear cell sarcoma was originally termed *melanoma of soft parts*. Despite its name, many CCSs lack clear cell cytoplasm and show epithelioid cells with abundant eosinophilic cytoplasm, vesicular nuclei, and prominent nucleoli, arranged in a nested or fascicular pattern. Despite sharing identical immunohistochemical phenotypes with melanoma, that is, positivity for melanocytic markers including S100, SOX10, HMB-45, and Melan-A, CCS is a distinct diagnostic entity owing to the presence of recurrent *EWSR1-ATF1* or *EWSR1-CREB1* fusions.[24–26] The list of differential diagnoses may also include perivascular epithelioid cell neoplasms (PEComa), which are also positive for HMB-45 but lack S100 and SOX10 staining, and gastrointestinal neuroectodermal tumor (GNET), formerly known as CCS-like tumor of the gastrointestinal tract, which shares the same fusions as CCS and is also S100- and SOX10-positive, but does not stain with melanocytic markers (HMB-45 and Melan-A). Of note, melanoma and CCS can be virtually impossible to distinguish without the aid of molecular tools to demonstrate the presence or absence of *EWSR1* fusions, which are characteristic of CCS.

In ABCs, numerous *USP6* gene rearrangements have been reported, the partners of which include *COL1A1*, *OMD*, *PAFAH1B1*, *RUNX2*, *SPARC*, *TRAP150*, *USP9X*, and *ZNF9*.[31–35] To our knowledge, *PTBP1* and *SLC38A2* are novel gene fusion partners of *USP6* in ABC that have not been reported to date. *PTBP1* encodes a ubiquitously expressed heterogeneous nuclear ribonucleoprotein,[45] while *SLC38A2* encodes a ubiquitously expressed amino acid transporter that responds to various hormonal stimuli to promote cell survival and metabolism.[46] In all cases, the entirety of the coding region of *USP6* is fused with an alternative promoter. The likely mechanism is upregulation of *USP6* gene transcription.[31]

About 20% to 30% of ABCs are secondary to a preexisting neoplasm, most frequently benign osseous or cartilaginous neoplasms, such as giant cell tumor of bone, chondroblastoma, or chondromyxoid fibroma, but a small subset could be associated with malignant bone tumors, most commonly osteosarcomas.[47] Cases where the cystic spaces are completely absent (so-called solid variant) could pose a diagnostic challenge in the differentiation of ABC from other giant cell–rich bone lesions.[48] Finally, in cases where atypical radiographic and/or histopathologic features are present, as illustrated in the second case in this report, ABC could sometimes be misdiagnosed as more aggressive tumors, particularly telangiectatic osteosarcomas.[49] In each of these above scenarios, the detection of a *USP6* gene

rearrangement, which is diagnostic of primary ABCs, readily resolves these diagnostic dilemmas.

TFG is a recurrent somatic fusion partner in a variety of tumor entities, including *TFG-ALK* in anaplastic large cell lymphoma,[50] *TFG-NTRK1* in thyroid papillary carcinoma,[51] *TFG-NR4A3/NOR1* in extraskeletal myxoid chondrosarcoma,[16,52] *TRK-GRP128* in clear cell renal cell carcinoma and Sézary syndrome.[53,54] The N-terminal sequence retained in *TFG* (*TRK*-fused gene) translocations contains a coiled-coil oligomerization domain,[48] which is required for oncogenic transformation of the fusion oncoprotein.[55,56] The usual configuration of these fusions involves *TFG* exon 4 or exon 5 fused to the partner. As such, our LDT includes GSPs designed to capture transcripts of *TFG* near these breakpoints. This allowed the detection of several *TFG-GPR128* fusions, which upon initial review would be concerning for a pathogenic fusion product, as this product is in-frame and includes the coiled-coiled oligomerization domain of the TFG protein. However, unlike recurrent, oncogenic *TFG* fusions, *TFG-GPR128* is due to a germline polymorphic copy number gain,[10,11,50–54] with the 5′ breakpoint located at the end of exon 3, instead of including all of exon 4 or 5 as observed in oncogenic fusions. To our knowledge, there are no reports of this polymorphism being detected with a targeted, somatic fusion NGS platform as part of routine clinical diagnostics. As clinical laboratories expand fusion-testing LDTs to include targeted panels, such as our SRCNGS, or more comprehensive assays such as whole transcriptome, there is a need to highlight recurrent polymorphic chimeric fusions, to reduce diagnostic errors or confusion.

Admittedly, a number of BST neoplasms could readily be identified with the use of newer immunohistochemical markers, some of which serve as a surrogate for underlying molecular alterations. Notable examples include STAT6 for solitary fibrous tumor, DOG1/c-kit for gastrointestinal stromal tumors, brachyury for chordomas, and MUC4 for low-grade fibromyxoid sarcoma/SEF.[57] In addition, FISH testing for *MDM2* gene amplification has become a crucial diagnostic tool for atypical lipomatous tumor/well-differentiated liposarcoma and dedifferentiated liposarcoma.[58] In this report, we place emphasis on entities that are still largely dependent on the detection of recurrent gene rearrangements for precise diagnosis. Further, in cases with limited material, especially those with a broad differential diagnosis, the use of this technology can replace the need to perform multiple immunohistochemical studies and/or FISH tests.

In summary, our custom 34-gene NGS-based LDT for detection of fusions demonstrated excellent diagnostic utility for the classification of BST neoplasms for both fusion-positive and fusion-negative cases. This technology is particularly useful for morphologically challenging cases and in the absence of prior knowledge of fusion partners.

We thank Giana D'Aleo, MS, Maureen A. Jakubowski, BS, MT, Robin Instone, BS, MB(ASCP), Jessica Spildener, MSPS, Rebecca Hutton, BS, Nicole Hamon, MSPS, MB(ASCP), Thomas Rose, MS, MT(ASCP), Christine Revay, BS, MB(ASCP), Ashlee Pimpas, MBA, MT(ASCP), and Kristen McDonnell, BS, MB(ASCP)CG, for excellent developmental, technical, and bioinformatics support of this laboratory-developed test.

References

1. Aman P. Fusion genes in solid tumors. *Semin Cancer Biol*. 1999;9(4):303–318.

2. Riggi N, Cironi L, Suvà ML, Stamenkovic I. Sarcomas: genetics, signalling, and cellular origins—Part 1: the fellowship of TET. *J Pathol*. 2007;213(1):4–20.

3. Suvà ML, Cironi L, Riggi N, Stamenkovic I. Sarcomas: genetics, signalling, and cellular origins—Part 2: TET-independent fusion proteins and receptor tyrosine kinase mutations. *J Pathol*. 2007;213(2):117–130.

4. Zhu G, Benayed R, Ho C, et al. Diagnosis of known sarcoma fusions and novel fusion partners by targeted RNA sequencing with identification of a recurrent ACTB-FOSB fusion in pseudomyogenic hemangioendothelioma. *Mod Pathol*. 2019;32(5):609–620.

5. Lam SW, Cleton-Jansen AM, Cleven AHG, et al. molecular analysis of gene fusions in bone and soft tissue tumors by anchored multiplex PCR-based targeted next-generation sequencing. *J Mol Diagn*. 2018;20(5):653–663.

6. Szurian K, Kashofer K, Liegl-Atzwanger B. Role of next-generation sequencing as a diagnostic tool for the evaluation of bone and soft-tissue tumors. *Pathobiology*. 2017;84(6):323–338.

7. Zheng Z, Liebers M, Zhelyazkova B, et al. Anchored multiplex PCR for targeted next-generation sequencing. *Nat Med*. 2014;20(12):1479–1484.

8. Abel HJ, Al-Kateb H, Cottrell CE, et al. Detection of gene rearrangements in targeted clinical next-generation sequencing. *J Mol Diagn*. 2014;16(4):405–417.

9. Kilpatrick SE, Reith JD, Rubin B. Ewing sarcoma and the history of similar and possibly related small round cell tumors: from whence have we come and where are we going? *Adv Anat Pathol*. 2018;25(5):314–326.

10. Chase A, Ernst T, Fiebig A, et al. TFG, a target of chromosome translocations in lymphoma and soft tissue tumors, fuses to GPR128 in healthy individuals. *Haematologica*. 2010;95(1):20–26.

11. Greger L, Su J, Rung J, et al. Tandem RNA chimeras contribute to transcriptome diversity in human population and are associated with intronic genetic variants. *PLoS One*. 2014;9(8):e104567.

12. Antonescu CR, Owosho AA, Zhang L, et al. Sarcomas with CIC-rearrangements are a distinct pathologic entity with aggressive outcome: a clinicopathologic and molecular study of 115 cases. *Am J Surg Pathol*. 2017;41(7):941–949.

13. Puls F, Niblett A, Marland G, et al. BCOR-CCNB3 (Ewing-like) sarcoma: a clinicopathologic analysis of 10 cases, in comparison with conventional Ewing sarcoma. *Am J Surg Pathol*. 2014;38(10):1307–1308.

14. Arnold MA, Schoenfield L, Limketkai BN, Arnold CA. Diagnostic pitfalls of differentiating desmoplastic small round cell tumor (DSRCT) from Wilms tumor (WT): overlapping morphologic and immunohistochemical features. *Am J Surg Pathol*. 2014;38(9):1220–1226.

15. Jin Y, Möller E, Nord KH, et al. Fusion of the AHRR and NCOA2 genes through a recurrent translocation t(5;8)(p15;q13) in soft tissue angiofibroma results in upregulation of aryl hydrocarbon receptor target genes. *Genes Chromosomes Cancer*. 2012;51(5):510–520.

16. Antonescu CR, Zhang L, Chang NE, et al. EWSR1-POU5F1 fusion in soft tissue myoepithelial tumors: a molecular analysis of sixty-six cases, including soft tissue, bone, and visceral lesions, showing common involvement of the EWSR1 gene. *Genes Chromosomes Cancer*. 2010;49(12):1114–1124.

17. Agaram NP, Zhang L, Sung YS, Singer S, Antonescu CR. Extraskeletal myxoid chondrosarcoma with non-EWSR1-NR4A3 variant fusions correlate with rhabdoid phenotype and high-grade morphology. *Hum Pathol*. 2014;45(5):1084–1091.

18. Rossi S, Szuhai K, Ijszenga M, et al. EWSR1-CREB1 and EWSR1-ATF1 fusion genes in angiomatoid fibrous histiocytoma. *Clin Cancer Res*. 2007;13(24):7322–7328.

19. Antonescu CR, Suurmeijer AJ, Zhang L, et al. Molecular characterization of inflammatory myofibroblastic tumors with frequent ALK and ROS1 gene fusions and rare novel RET rearrangement. *Am J Surg Pathol*. 2015;39(7):957–967.

20. Arbajian E, Puls F, Magnusson L, et al. Recurrent EWSR1-CREB3L1 gene fusions in sclerosing epithelioid fibrosarcoma. *Am J Surg Pathol*. 2014;38(6):801–808.

21. Suurmeijer AJH, Song W, Sung YS, et al. Novel recurrent PHF1-TFE3 fusions in ossifying fibromyxoid tumors. *Genes Chromosomes Cancer*. 2019;58(9):643–649.

22. Patel KU, Szabo SS, Hernandez VS, et al. Dermatofibrosarcoma protuberans COL1A1-PDGFB fusion is identified in virtually all dermatofibrosarcoma protuberans cases when investigated by newly developed multiplex reverse transcription polymerase chain reaction and fluorescence in situ hybridization assays. *Hum Pathol*. 2008;39(2):184–193.

23. Le Guellec S, Decouvelaere AV, Filleron T, et al. Malignant peripheral nerve sheath tumor is a challenging diagnosis: a systematic pathology review, immunohistochemistry, and molecular analysis in 160 patients from the French Sarcoma Group Database. *Am J Surg Pathol*. 2016;40(7):896–908.

24. Wang WL, Mayordomo E, Zhang W, et al. Detection and characterization of EWSR1/ATF1 and EWSR1/CREB1 chimeric transcripts in clear cell sarcoma (melanoma of soft parts). *Mod Pathol*. 2009;22(9):1201–1209.

25. Graadt van Roggen JF, Mooi WJ, Hogendoorn PC. Clear cell sarcoma of tendons and aponeuroses (malignant melanoma of soft parts) and cutaneous melanoma: exploring the histogenetic relationship between these two clinicopathological entities. *J Pathol*. 1998;186(1):3–7.

26. Langezaal SM, Graadt van Roggen JF, Cleton-Jansen AM, Baelde JJ, Hogendoorn PC. Malignant melanoma is genetically distinct from clear cell sarcoma of tendons and aponeurosis (malignant melanoma of soft parts). *Br J Cancer*. 2001;84(4):535–538.

27. Antonescu CR, Elahi A, Humphrey M, et al. Specificity of TLS-CHOP rearrangement for classic myxoid/round cell liposarcoma: absence in predom-

inantly myxoid well-differentiated liposarcomas. *J Mol Diagn*. 2000;2(3):132–138.

28. Downes KA, Goldblum JR, Montgomery EA, Fisher C. Pleomorphic liposarcoma: a clinicopathologic analysis of 19 cases. *Mod Pathol*. 2001;14(3):179–184.

29. Wang L, Motoi T, Khanin R, et al. Identification of a novel, recurrent HEY1-NCOA2 fusion in mesenchymal chondrosarcoma based on a genome-wide screen of exon-level expression data. *Genes Chromosomes Cancer*. 2012;51(2):127–139.

30. Righi A, Gambarotti M, Longo S, et al. Small cell osteosarcoma: clinicopathologic, immunohistochemical, and molecular analysis of 36 cases. *Am J Surg Pathol*. 2015;39(5):691–699.

31. Oliveira AM, Perez-Atayde AR, Dal Cin P, et al. Aneurysmal bone cyst variant translocations upregulate USP6 transcription by promoter swapping with the ZNF9, COL1A1, TRAP150, and OMD genes. *Oncogene*. 2005;24(21):3419–3426.

32. Warren M, Xu D, Li X. Gene fusions PAFAH1B1-USP6 and RUNX2-USP6 in aneurysmal bone cysts identified by next generation sequencing. *Cancer Genet*. 2017;212-213:13–18.

33. Šekoranja D, Boštjancic E, Salapura V, Mavcic B, Pižem J. Primary aneurysmal bone cyst with a novel SPARC-USP6 translocation identified by next-generation sequencing. *Cancer Genet*. 2018;228-229:12–16.

34. Guseva NV, Jaber O, Tanas MR, et al. Anchored multiplex PCR for targeted next-generation sequencing reveals recurrent and novel USP6 fusions and upregulation of USP6 expression in aneurysmal bone cyst. *Genes Chromosomes Cancer*. 2017;56(4):266–277.

35. Blackburn PR, Davila JI, Jackson RA, et al. RNA sequencing identifies a novel USP9X-USP6 promoter swap gene fusion in a primary aneurysmal bone cyst. *Genes Chromosomes Cancer*. 2019;58(8):589–594.

36. Morohoshi F, Arai K, Takahashi EI, Tanigami A, Ohki M. Cloning and mapping of a human RBP56 gene encoding a putative RNA binding protein similar to FUS/TLS and EWS proteins. *Genomics*. 1996;38(1):51–57.

37. Stolow DT, Haynes SR. Cabeza, a Drosophila gene encoding a novel RNA binding protein, shares homology with EWS and TLS, two genes involved in human sarcoma formation. *Nucleic Acids Res*. 1995;23(5):835–843.

38. Arvand A, Denny CT. Biology of EWS/ETS fusions in Ewing's family tumors. *Oncogene*. 2001;20(40):5747–5754.

39. Romeo S, Dei Tos AP. Soft tissue tumors associated with EWSR1 translocation. *Virchows Arch*. 2010;456(2):219–234.

40. Paronetto MP. Ewing sarcoma protein: a key player in human cancer. *Int J Cell Biol*. 2013;2013:642853.

41. Thway K, Fisher C. Tumors with EWSR1-CREB1 and EWSR1-ATF1 fusions: the current status. *Am J Surg Pathol*. 2012;36(7):e1–e11.

42. Cleven AH, Sannaa GA, Briaire-de Bruijn I, et al. Loss of H3K27 tri-methylation is a diagnostic marker for malignant peripheral nerve sheath tumors and an indicator for an inferior survival. *Mod Pathol*. 2016;29(6):582–590.

43. Le Guellec S, Macagno N, Velasco V, et al. Loss of H3K27 trimethylation is not suitable for distinguishing malignant peripheral nerve sheath tumor from melanoma: a study of 387 cases including mimicking lesions. *Mod Pathol*. 2017;30(12):1677–1687.

44. Marchione DM, Lisby A, Viaene AN, et al. Histone H3K27 dimethyl loss is highly specific for malignant peripheral nerve sheath tumor and distinguishes true PRC2 loss from isolated H3K27 trimethyl loss. *Mod Pathol*. 2019;32(10):1434–1446.

45. Romanelli MG, Lorenzi P, Avesani F, Morandi C. Functional characterization of the ribonucleoprotein, PTB-binding 1/Raver1 promoter region. *Gene*. 2007;405(1-2):79–87.

46. Menchini RJ, Chaudhry FA. Multifaceted regulation of the system A transporter SLC38A2 suggests nanoscale regulation of amino acid metabolism and cellular signaling. *Neuropharmacology*. 2019;161:107789.

47. Sanerkin NG, Mott MG, Roylance J. An unusual intraosseous lesion with fibroblastic, osteoclastic, osteoblastic, aneurysmal and fibromyxoid elements: "solid" variant of aneurismal bone cyst. *Cancer*. 1983;51(12):2278–2286.

48. Martinez V, Sissons HA. Aneurysmal bone cyst: a review of 123 cases including primary lesions and those secondary to other bone pathology. *Cancer*. 1988;61(11):2291–2304.

49. Huvos AG, Rosen G, Bretsky SS, Butler A. Telangiectatic osteogenic sarcoma: a clinicopathologic study of 124 patients. *Cancer*. 1982;49(8):1679–1689.

50. Hernández L, Beà S, Bellosillo B, et al. Diversity of genomic breakpoints in TFG-ALK translocations in anaplastic large cell lymphomas: identification of a new TFG-ALK(XL) chimeric gene with transforming activity. *Am J Pathol*. 2002;160(4):1487–1494.

51. Mencinger M, Panagopoulos I, Andreasson P, Lassen C, Mitelman F, Aman P. Characterization and chromosomal mapping of the human TFG gene involved in thyroid carcinoma. *Genomics*. 1997;41(3):327–331.

52. Hisaoka M, Ishida T, Imamura T, Hashimoto H. TFG is a novel fusion partner of NOR1 in extraskeletal myxoid chondrosarcoma. *Genes Chromosomes Cancer*. 2004;40(4):325–328.

53. Cancer Genome Atlas Research Network. Comprehensive molecular characterization of clear cell renal cell carcinoma. *Nature*. 2013;499(7456):43–49.

54. Iżykowska K, Przybylski GK, Gand C, et al. Genetic rearrangements result in altered gene expression and novel fusion transcripts in Sézary syndrome. *Oncotarget*. 2017;8(24):39627–39639.

55. Greco A, Mariani C, Miranda C, et al. The DNA rearrangement that generates the TRK-T3 oncogene involves a novel gene on chromosome 3 whose product has a potential coiled-coil domain. *Mol Cell Biol*. 1995;15(11):6118–6127.

56. Greco A, Fusetti L, Miranda C, et al. Role of the TFG N-terminus and coiled-coil domain in the transforming activity of the thyroid TRK-T3 oncogene. *Oncogene*. 1998;16(6):809–816.

57. Wei S, Henderson-Jackson E, Qian X, Bui MM. Soft tissue tumor immunohistochemistry update: illustrative examples of diagnostic pearls to avoid pitfalls. *Arch Pathol Lab Med*. 2017;141(8):1072–1091.

58. Clay MR, Martinez AP, Weiss SW, Edgar MA. MDM2 amplification in problematic lipomatous tumors: analysis of FISH testing criteria. *Am J Surg Pathol*. 2015;39(10):1433–1439.

59. Krzywinski M, Schein J, Birol I, et al. Circos: an information aesthetic for comparative genomics. *Genome Res*. 2009;19(9):1639–1645.